CHEMISTRY OF MATERIALS
Review

Chem. Mater. **2011,** *23,* 631–645 631
DOI:10.1021/cm102402t

Probing Hopping Conduction in Conjugated Molecular Wires Connected to Metal Electrodes†

Liang Luo, Seong Ho Choi, and C. Daniel Frisbie*

Department of Chemical Engineering and Materials Science, University of Minnesota, Minneapolis, Minnesota 55455, United States

Received August 20, 2010. Revised Manuscript Received October 2, 2010

Understanding electrical transport processes in molecules connected between metal electrodes is a central focus in the field of molecular electronics and is important for both potential applications and fundamental research purposes. This short review summarizes recent progress in assembling and measuring strategies for long conjugated molecular wires within molecular junctions, and introduces several new in situ methods to prepare molecular wires connected to electrodes. Following a brief introduction to charge transport mechanisms, particular examples of molecular wires in the recent literature are presented to discuss the influence of molecular length, temperature, and applied voltage on the transport properties with emphasis on the tunneling-to-hopping transition. The review concludes with an outlook on future hopping transport experiments in long conjugated molecular wires.

1. Introduction

Molecular wires are π-conjugated molecules that can transport charge efficiently over long distances. By "long" we mean lengths longer than typical tunneling distances (~1−4 nm), but tiny in comparison to length scales in the macroscopic world. In principle, the conduction properties of molecular wires can be measured by connecting molecules between electrodes forming a "molecular junction", Figure 1. Multiple strategies for forming molecular junctions have been reported over the past 15 years and the current−voltage ($I-V$) characteristics of a spectrum of conjugated molecules have been measured.[1−5] Such experiments are motivated by both fundamental considerations and potential applications. From a fundamental perspective, the most intriguing prospect is to understand the connection between molecular architecture and the conduction properties of molecular wires. For example, one can discover how the resistance of a molecular wire depends on the bonding architecture and corresponding electronic energy levels in the wire backbone (Figure 1), or how the resistance scales with wire length (e.g., how similar is a molecular wire to a nanoscopic copper wire?). The information gained from such experiments may one day influence the molecular design of conjugated polymers, also known as polymer semiconductors, for improved performance in plastic solar cells,[6,7] light-emitting diodes,[8,9] or transistors,[10,11] thus linking fundamental science with applications. Also in relation to applications, the development of molecular wires and switches is a central goal for the field of molecular electronics, where the aim is to exploit the properties of molecules for nanoscale electronics.[12−17]

In most molecular junctions reported to date, the component molecules are less than 4 nm in length. For such short molecules, the predominant transport mechanism in the junctions is metal-to-metal tunneling, i.e., the electron crosses the junction in a single step and has no appreciable residence time on the molecule. There are some notable exceptions to this, for example junctions exhibiting Coulomb blockade behavior in which charge crosses the junction in two hops, i.e., metal-to-molecule and molecule-to-metal.[18,19] Understanding tunneling transport in molecular junctions based on short molecules continues to be an important research area.

The focus of this short review, however, is on direct current (DC) electrical conduction in junctions incorporating molecules longer than ~4 nm in which charges are injected into molecular orbitals and are driven along the molecular backbone by an applied field − the so-called multistep hopping transport regime. The hopping regime is much less explored and offers exciting opportunities to connect molecular junction results to more macroscopic measurements of charge transport in technologically relevant thin films of conjugated polymers where the relative roles of intra- versus intermolecular charge hopping are not well understood. It is also likely that structure−transport relationships in the hopping regime will significantly diverge from results obtained in the tunneling (short molecule) domain and the new findings may substantially impact the fields of molecular and organic electronics. Because DC hopping has not been well explored in molecular junctions, the number of papers in the literature on the topic is currently rather small, perhaps ~20.[20−43] However, there are a number of excellent

† Accepted as part of the "Special Issue on π-Functional Materials".
*Corresponding author. E-mail: frisbie@umn.edu.

Published on Web 10/26/2010

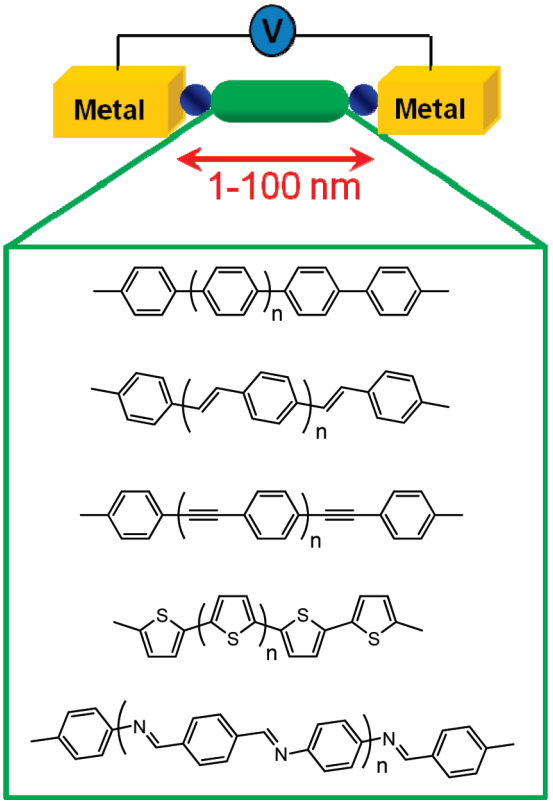

Figure 1. Schematic representation of long conjugated molecular wires connected between metal electrodes in a molecular junction.

reviews published in recent years regarding many other aspects of molecular junctions, such as experimental strategies,[4,5,44] single-molecule devices,[17,45] electrochemical approaches,[46,47] and theoretical modeling;[14,48] these topics will not be the focus of this article.

In considering the literature, it is important to acknowledge that DC conduction measurements on molecules benefit tremendously from decades of prior work on solution electron transfer in so-called donor−bridge−acceptor (D−B−A) molecules.[49−54] The prior electron transfer work has revealed and quantified the key factors associated with both the tunneling and multistep hopping regimes in molecules, including the important role played by the length of the molecular bridge.[55−57] The significance of this prior work in which electron transfer rate constants have been quantitatively related to free energy changes and molecular reorganization energies cannot be overstated.[51,58] However, there are substantial differences between molecular junction and intramolecular solution electron transfer experiments.[59] The most obvious differences are the presence of external electric fields and the metal-molecule contacts in molecular junctions. Injection of charge from metals into molecules naturally depends on image forces and dipoles that can exist at metal−molecule interfaces, as well as on metal−molecule coupling and the energetic position of the Fermi level with respect to the molecular orbitals.[59−61] In addition, the field between the electrodes provides a substantial driving force for conduction that can impact not only the average hopping rate but even the number of electrons that transport across a junction. It seems best to view the solution electron transfer and solid-state DC conduction measurements as complementary approaches to the problem of electron transport in molecules.

2. Assembly Strategies for Long Molecular Wires between Metal Contacts

To date various reliable and efficient methods have been developed to assemble molecular wires into molecular junctions. However, given the complexities of adsorbing to metal surfaces while controlling orientation, development of methods to position a long molecule between metal contacts remains a fundamental challenge. One can synthesize wire components ex situ and insert such preprepared molecular wires between electrodes, as will be described in section 2.1. Sections 2.2 and 2.3 discuss another in situ approach, namely stepwise synthesis of molecular wires on electrodes. By this strategy, long molecular wires with different lengths can be synthesized and assembled with controlled orientation into molecular junctions.

2.1. Assembling Long Preprepared Molecular Wires in Molecular Junctions. Assembling preprepared molecular wires into molecular junctions is a strategy typically employed for short molecular wires (i.e., length <4 nm). However, there are a few reports on assembling preprepared long molecular wires between metal electrodes. Bjørnholm and co-workers have fabricated a single *p*-phenylenevinylene oligomer containing five benzene rings (Figure 2A) by chemical vapor deposition into an electrode nanogap to form a single-electron transistor.[19] Derivatives of oligo(*p*-phenylene ethynylene) (OPE) as long as 18 nm, as shown in Figure 2B, have also been connected between nanogap electrodes by Hu and coworkers.[62] Ashwell, et al.[63] reported that an arylene-ethynylene molecular wire (7 nm in length, Figure 2C) can form self-assembled monolayers (SAMs) on Au surfaces, and the second contact was provided by a scanning tunneling microscopy (STM) tip.

By assembling molecular wires of different lengths within molecular junctions, the electrical properties of functional conjugated molecular wires can be examined as a function of length.[31,35,39,40,64] Tada and co-workers have assembled oligothiophenes of 5-, 8-, 11-, and 14-mers (Figure 3A, $m=1-4$) into junctions and measured their electrical conductance individually.[40] Later, they extended the molecular wire series to a 23-mer, where $m=7$.[35] The longest 23-mer oligothiophene prepared in the molecular junction enabled an investigation of the conductance mechanism for lengths of up to 9 nm. Very recently, Tao et al.[64] studied the charge transport characteristics of a family of long conjugated molecular wires with length up to 9.4 nm using the STM break junction technique (Figure 3B, $n=1-4$). Wang and colleagues investigated the charge-transport mechanism of OPE wires with lengths ranging from 0.98 to 5.11 nm (Figure 3C).[31] The OPE wires were assembled into STM break junctions (see section 3), and can also form SAMs on Au substrates.

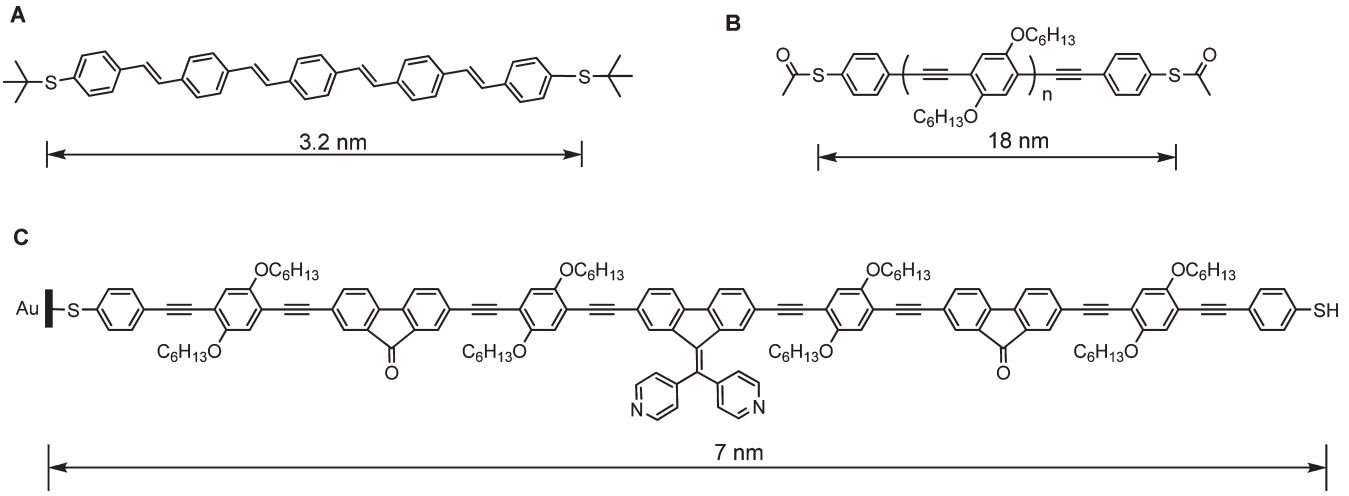

Figure 2. Selected long conjugated molecular wires that can be assembled between metal electrodes.[19,62,63].

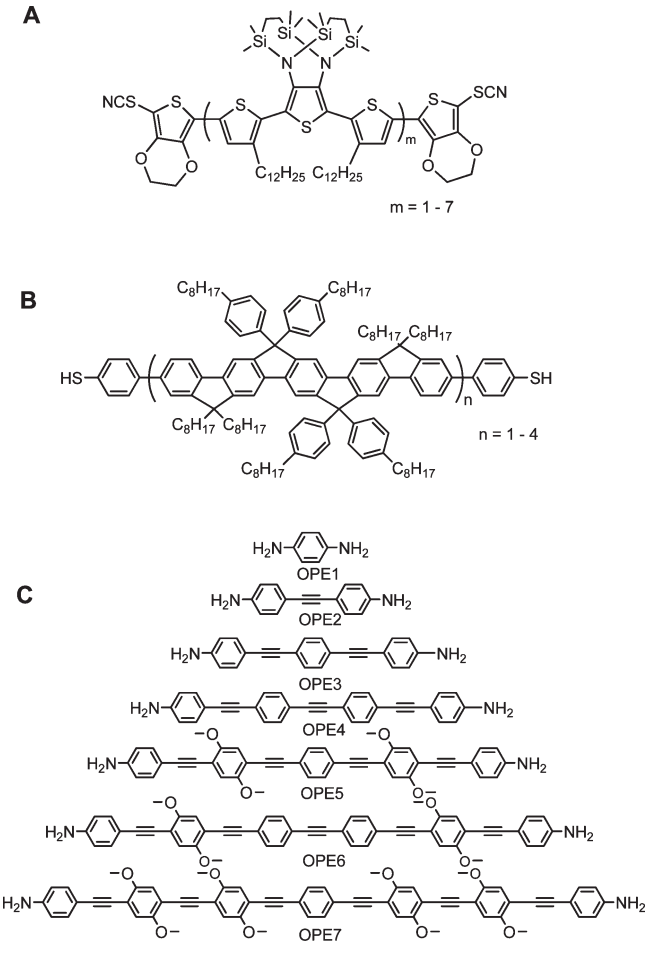

Figure 3. (A) Oligothiophenes with different repeat units contacted in STM break junctions. Reproduced with permission from ref 35. Copyright 2009 the Japan Society of Applied Physics. (B) Family of long conjugated molecular wires assembled in STM break junctions. Reproduced with permission from ref 64. Copyright 2010 American Chemical Society. (C) OPE with different lengths that can form SAMs on Au surfaces. Reproduced with permission from ref 31. Copyright 2009 American Chemical Society.

In addition, single molecule junctions based on extra long conjugated molecular wires with lengths greater that 100 nm were fabricated by contacting a single polyfluorene chain adsorbed on an Au(111) surface with an STM tip, as demonstrated in Figure 4.[65] The tip was used to pull the wire off the surface and the conductance was measured as a function of distance between the STM tip and the Au surface. However, the low-bias conductance of the molecular wire was too low to be detected when the tip−surface distance was beyond 4 nm.

2.2. Stepwise Growth of Long Conjugated Molecular Wires on Electrodes. Although long conjugated molecular wires can be assembled directly between metal contacts, their extended length and rigid backbones result in severe solubility problems and increased synthetic challenges. In addition, long molecules often do not adsorb to metal surfaces in an oriented, organized fashion, which further impedes junction formation. An alternative strategy is to synthesize molecular wires from one electrode using stepwise condensation chemistry. This approach solves the solubility and assembly problems and it also offers a convenient way to control wire length. The molecular junction can be formed by bringing a second electrode, such as a metal-coated atomic force microscopy (AFM) tip, into contact with the other end of the wires.

Oligophenyleneimine (OPI) wires bound to Au substrates were prepared recently[27] by Choi and co-workers, following a stepwise synthesis procedure originally described by Rosink, et. al,[66] as exhibited in Figure 5A. The growth procedure begins by adsorption of a SAM of 4-aminothiophenol on Au. OPI wire precursors (OPI-p) wires were then grown by stepwise imination, with alternate addition of dialdehyde and diamine blocks. Each OPI-p wire terminated with $-NH_2$ or $-CHO$ groups was end-capped with benzaldehyde or aniline respectively to provide a consistent terminal group throughout all OPI wires, which facilitated reproducible electrical characterization. Long conjugated OPI molecules were readily built by this stepwise methodology, with controlled orientation and approximately constant surface density. Reflection−absorption FTIR (Figure 5B) was used to confirm the imination mechanism and the completion of each reaction.

The preparation of OPI wires ranging in length from 1.5 to 7.3 nm enabled a detailed characterization of their

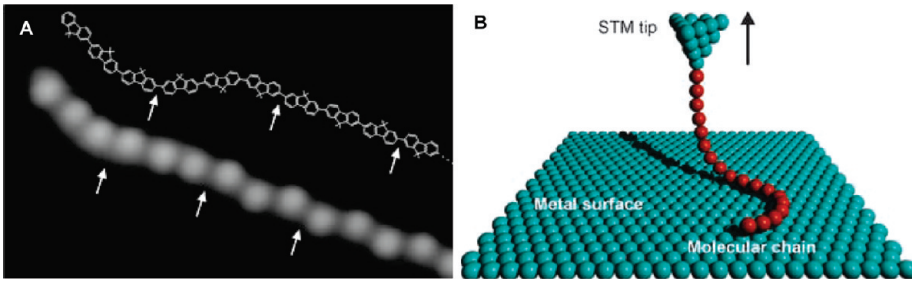

Figure 4. (A) STM image (5.9 nm × 3.6 nm) of a single polyflurene wire with its chemical structure superimposed (using a different scaling). (B) Scheme of the chain pulling procedure: After contacting a molecular chain to the STM tip, it can be lifted from the surface in a ropelike manner upon retraction because of its flexibility and weak interaction with the substrate. Reproduced with permission from ref 65. Copyright 2009 the American Association for the Advancement of Science.

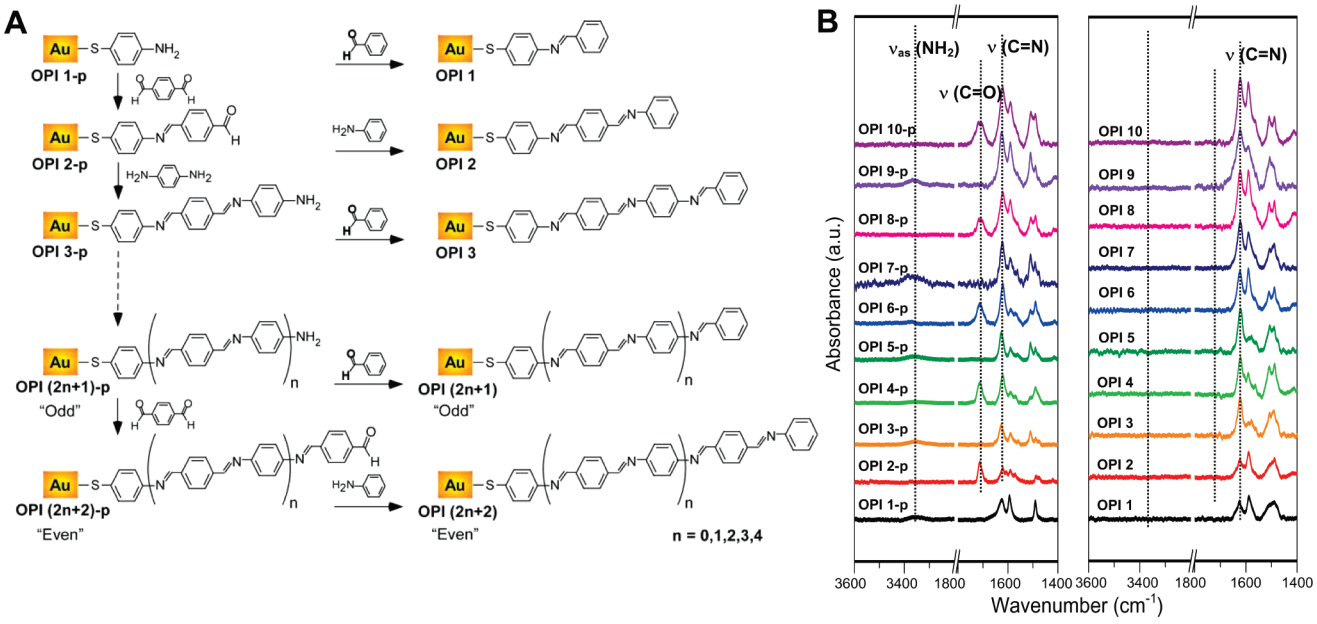

Figure 5. (A) Stepwise synthesis of OPI wires on an Au electrode. (B) Corresponding reflection−absorption FTIR spectra. Reproduced with permission from ref 27. Copyright 2008 American Association for the Advancement of Science.

transport properties as a function of molecular length and other factors, which will be further discussed in section 4. By this stepwise imine chemistry, one can synthesize a variety of long conjugated molecular wires bound to metal surfaces using different molecular building blocks, as exhibited in Figure 6. Specifically, oligonaphthalene-fluoreneimine (ONI) wires with lengths up to 10 nm have also been prepared by alternate addition of naphthalene dialdehyde and fluorene diamine blocks.[36] Oligoimines prepared using tetrathiafulvalene dialdehyde and pyromelliticdiimide diamine as building blocks result in even longer wires (20 nm) and more efficient charge transport caused by the intrachain donor−acceptor communication.[43]

The technique of stepwise growth of long conjugated molecular wires on electrodes has attracted more interest recently, as several different reaction schemes can be employed.[67−69] Figure 7 lists two more recent examples of long conjugated molecular wires grown on electrodes iteratively. Using stepwise copper(I) catalyzed alkyne−azide cycloaddition, so-called "click" chemistry,[70] oligophenylenetriazole (OPT) wires on Au substrates were prepared by Luo, et al. with controlled length and orientation (Figure 7A).[37] The prepared all-aromatic molecular wires provide more efficient transport than the oligoimine wires. In addition, Rampi and co-workers[34] have reported the preparation and characterization of a series of highly conductive metal-coordinating molecular wires, up to 40 nm in length, by alternate incorporation of metal ions and terpyridyl ligands, Figure 7B.

Lindsey and co-workers have developed a stepwise synthesis of oligomers of porphyrin-imide architectures on Si surfaces.[71] After forming a base monolayer of triallyl-funtionalized porphyrin (**P-a** in Figure 8), the wire was grown by successive reactions between dianhydride (BPTC) and dianiline porphyrin derivative (**2** in Figure 8). This repeated process led to polyimide wires covalently linked to the porphyrin base layer, composed of up to 5 porphyrins. The attractive aspects of the method are the high thermal stability (~400 °C) and redox stability of the corresponding imide oligomers, which the authors note is essential for use in semiconductor fabrication processes.

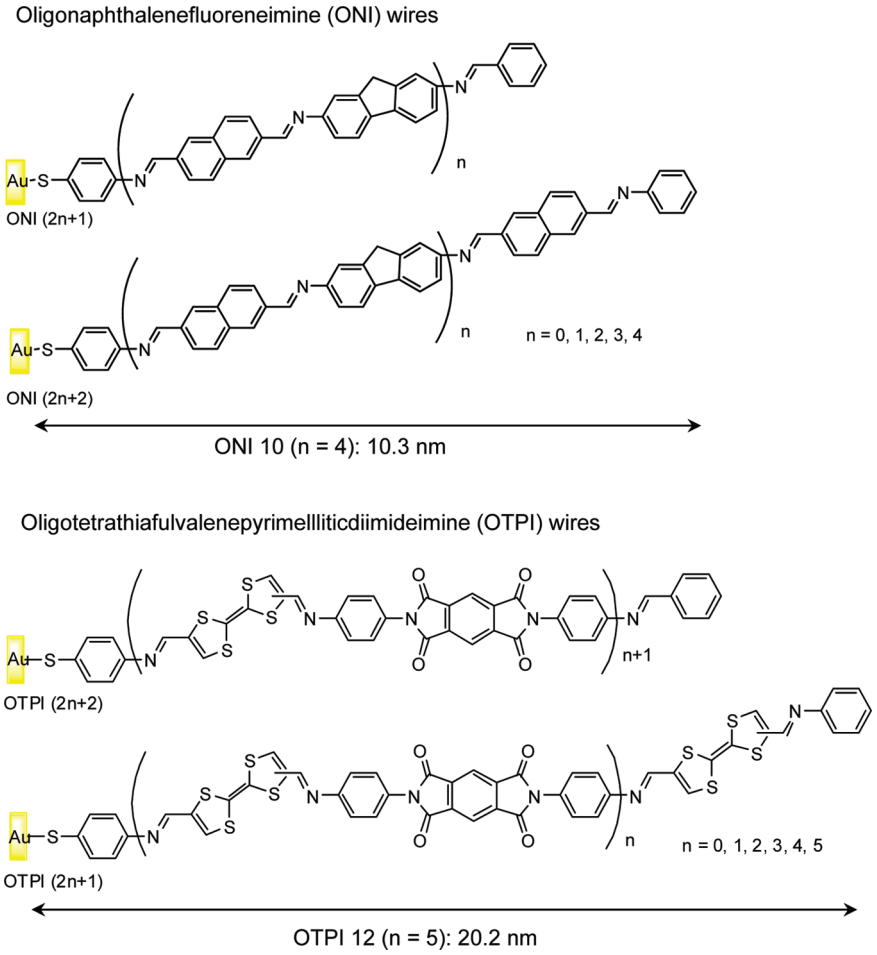

Figure 6. ONI[36] and OTPI[43] wires prepared by stepwise imination on Au substrates.

2.3. Interconnecting Both Electrodes by In situ Stepwise Synthesis of Molecular Wires. The in situ stepwise growth of molecular wires can also start simultaneously from both electrodes of a nanogap. The two elongated wire components from each electrode interconnect each other eventually, bridging the nanogap to form a molecular junction. This approach facilitates the fabrication of bi-end-functionalized molecular wires with extended length, where identical surface-linker groups are attached to opposite electrodes.[72−75] In principle, the contacts are more symmetric than in the single electrode stepwise growth approach.

Using this interconnect method, Taniguchi and co-workers have wired two electrodes with oligophenylenevinylene derivatives (Figure 9A).[73] The wire, synthesized by stepwise Suzuki coupling, has a length of 30 nm. Nuckolls et al.[74] integrated chemical synthesis with the formation of a molecular junction to allow the in situ construction of three-component molecular wires (Figure 9B). More recently, Mirkin and co-workers[75] have developed a general approach to form long wire junctions by interlinking nanogaps of various dimensions, as shown in Figure 9C. The nanogap electrodes were fabricated by on-wire lithography (OWL) with different gap sizes in the range of several nanometers. The acetylene-functionalized electrodes were sequentially interconnected by oligo triazole-interlinked fluorenes with required lengths, formed in situ by stepwise click chemistry.

3. Measurement Strategies

The measured electrical behavior of molecular wires depends not only on the molecules themselves, but also on the properties of the electrodes and on the atomic-scale molecule-electrode contact geometry. Figure 10 illustrates the main strategies that have been developed for the electrical measurement of nanoscale molecular junctions.[4,5,44] Molecular junctions can be divided into two broad categories: single-molecule versus molecular ensemble strategies. Single-molecule approaches include STM and break junctions, Figures 10A, B. Ensemble junctions include conducting probe AFM (CP-AFM), crossed wire junctions, and other bulk and nano electrodes that sandwich molecular films, as demonstrated in Figures 10C−F.

In the STM approach, depicted in Figure 10A, an atomically sharp metallic STM tip is employed to contact single molecules in a SAM on a metal substrate. The conjugated molecules of interest (red in Figure 10A) are usually embedded into a matrix of insulating molecules (e.g., alkanes), and one can observe much higher current through the conjugated molecular wires than through the surrounding matrix.[4,76−78] Single molecules can also be electronically contacted in "break junctions", Figure 10B.[4,44,79,80] In break junctions, molecules from

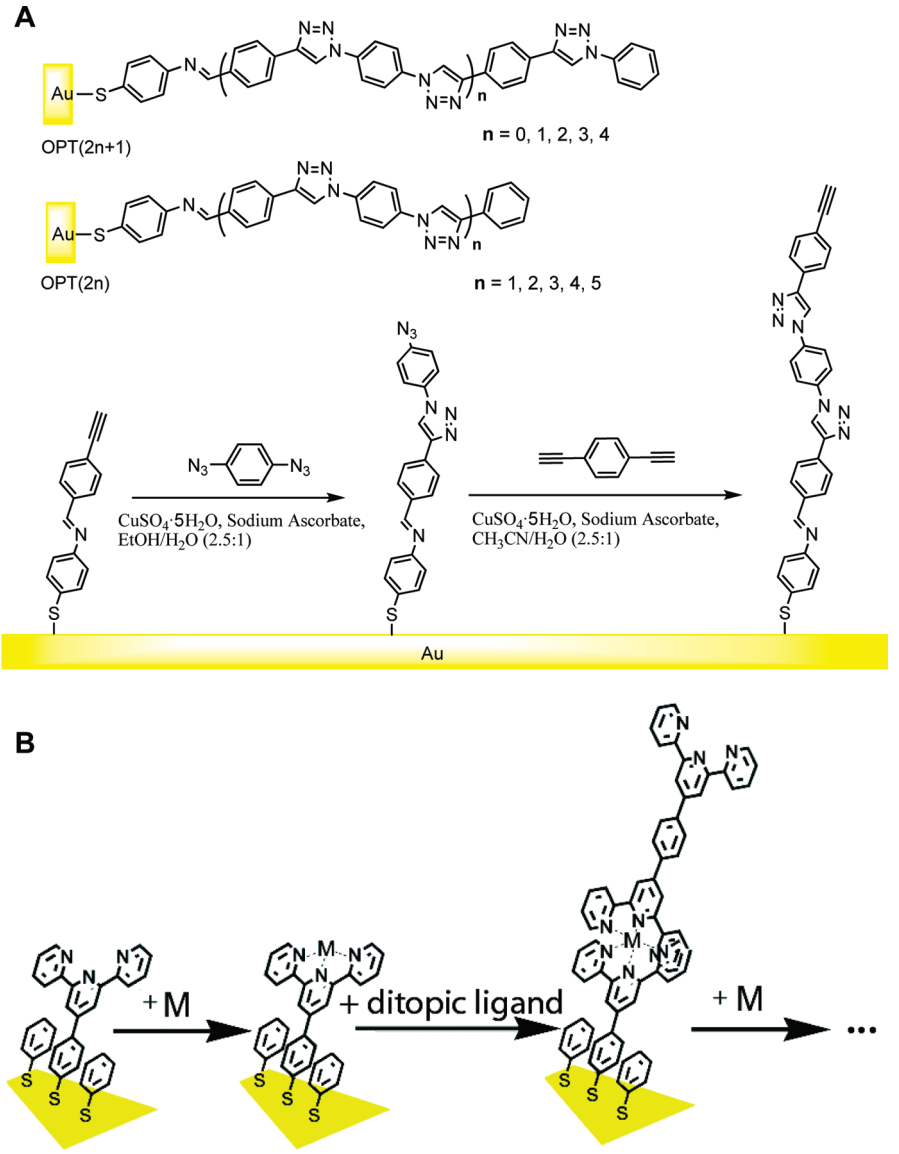

Figure 7. (A) Stepwise click chemistry applied to synthesize OPT wires on Au substrates. Modified with permission from ref 37. Copyright 2010 American Chemical Society. (B) Stepwise assembly of metal-containing molecular wires on Au surfaces. Reproduced with permission from ref 34. Copyright 2009 Nature Publishing Group.

a surrounding solution adsorb in a metal nanogap freshly created by stretching a thin wire[79,81] or by retracting a metal STM tip from a metal surface.[80,82]

Single molecule junctions are conceptually attractive because they represent an extreme limit, namely one molecule between two nanoscale contacts. Also, the problems of intermolecular interactions and their impact on the wire resistance are removed. However, it can be difficult to obtain data on very long molecular wires because of signal-to-noise issues (i.e., long molecules are more resistive). In addition, the observed conduction of single molecules depends strongly on the contact geometry and conformation, and one has to average out this contact effect by measuring many single-molecule devices.

Ensemble measurements, on the contrary, suffer less from signal-to-noise issues and allow measurements on arbitrarily long molecular wires. This is because the ensemble generally consists of $\sim 1 \times 10^2$ to $\sim 1 \times 10^{13}$ parallel aligned molecules, which increases the current at a given voltage. The enhancement in signal however comes somewhat at the expense of junction simplicity, i.e., intermolecular interactions are now important and the observed $I-V$ characteristics reflect average behavior of all molecules in the junction. On the other hand, ensemble junctions are more amenable to structural and chemical characterization methods (e.g., FTIR, UV−vis, XPS, etc.) than single molecule junctions, and this can aid interpretation of the electrical data.

A particularly convenient and reproducible ensemble method is the CP-AFM approach in which a metal-coated AFM tip is brought in direct contact with a SAM of molecular wires at a controlled contact force, Figure 10C.[83−93] Sweeping the tip voltage allows measurement of the $I-V$ characteristics of the molecular wire monolayer in the junction. The contact area of the junction is on the order of 10 nm^2, making it particularly suitable for the electrical measurement of the SAMs: the number of probed molecules ($\sim$100)[94] reduces the

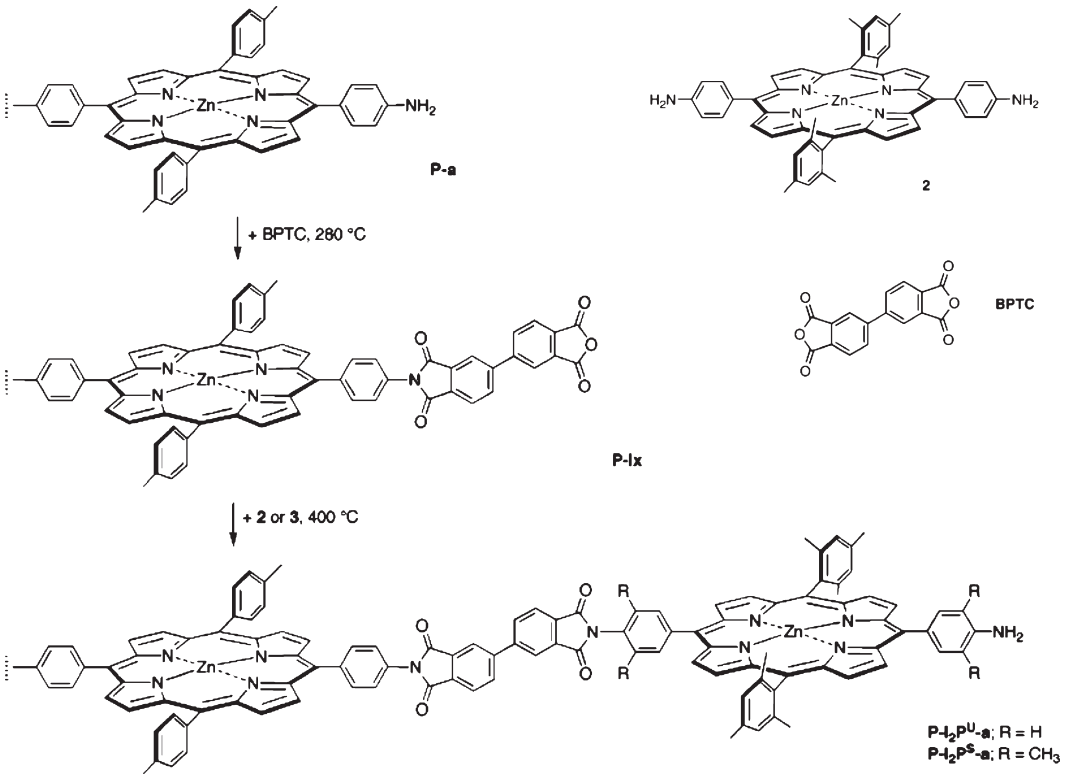

Figure 8. Stepwise formation of multiporphyrin-imide architectures on Si (100). Reproduced with permission from ref 71. Copyright 2006 the American Chemical Society.

probability of electrical shorts and the impact of defects, but can still provide electrical properties of a statistical number of molecules. In addition, CP-AFM offers significant experimental flexibility in that the tip and substrate can be coated with different metals, which allows assessment of the role of different metal work functions on junction $I-V$ behavior.

The $I-V$ characteristics of wire ensembles based on SAMs can also be measured in crossed-wire tunnel junctions (Figure 10D)[78,95,96] or in mercury-drop junctions (Figure 10E).[97−99] The crossed-wire junction is formed by gentle contact of two crossing 10 μm diameter metal wires, one of which is coated with a SAM of the test molecule. The junction contains $\sim 1 \times 10^3$ molecules with a high degree of control and choice of metal.[95] In comparison, the mercury-drop junction, formed by contacting a SAM on metal with a hanging mercury drop, has a much larger contact area (1.0 mm in diameter) and contains 1×10^{11} to 1×10^{13} molecules.[99] More recent technology for the fabrication of large area ensemble devices (ranging from 10 to 100 μm in diameter) incorporates a conducting polymer (PEDOT:PSS) as a top electrode,[100,101] the cross-section of which is depicted in Figure 10F. The use of conducting PEDOT:PSS not only ensures a good contact of the measurement probes to the device, but also prevents short circuits, a result that is attributed to poor penetration of the PEDOT:PSS macromolecules into the densely packed SAMs.[102] In another technique that eliminates the penetration problem of ensemble junctions, namely surface-diffusion-mediated deposition,[103] metals are deposited adjacent to the molecular layer with a distance of ~50 nm, and then diffuse onto the molecular layer softly to form the metallic contact.

The role of intermolecular interactions and defects remains an important and often open-ended aspect for interpreting ensemble junction $I-V$ data. Domains with high defect densities can exist in most monolayers, which may affect averaged results or cause nanoscopic electrical shorts. In addition, intermolecular interactions within densely packed monolayers can also result in significant changes in the energies of the molecular orbitals involved in conduction. Collectively, both single-molecule and ensemble measurements have advantages and limitations, and it is crucial to recognize these aspects before evaluating the results obtained by each method.

4. Probing Charge Transport in Conjugated Molecular Wires: Tunneling versus Hopping

4.1. Tunneling and Hopping Transport Mechanisms in Molecular Junctions. Reviewing basic charge transport mechanisms is required to understand the broad spectrum of $I-V$ behavior exhibited in molecular junctions. It is well-known that for both saturated molecules and sufficiently short conjugated molecules connected to electrodes, electrons can tunnel between the two contacts. In this situation, the junction resistance increases exponentially with molecular length and is only weakly temperature dependent.[14,85,93,94] The tunneling mechanism is often "non-resonant" in that the tunneling electron energies are not precisely matched with the molecular orbital energies. For longer conjugated molecular wires at

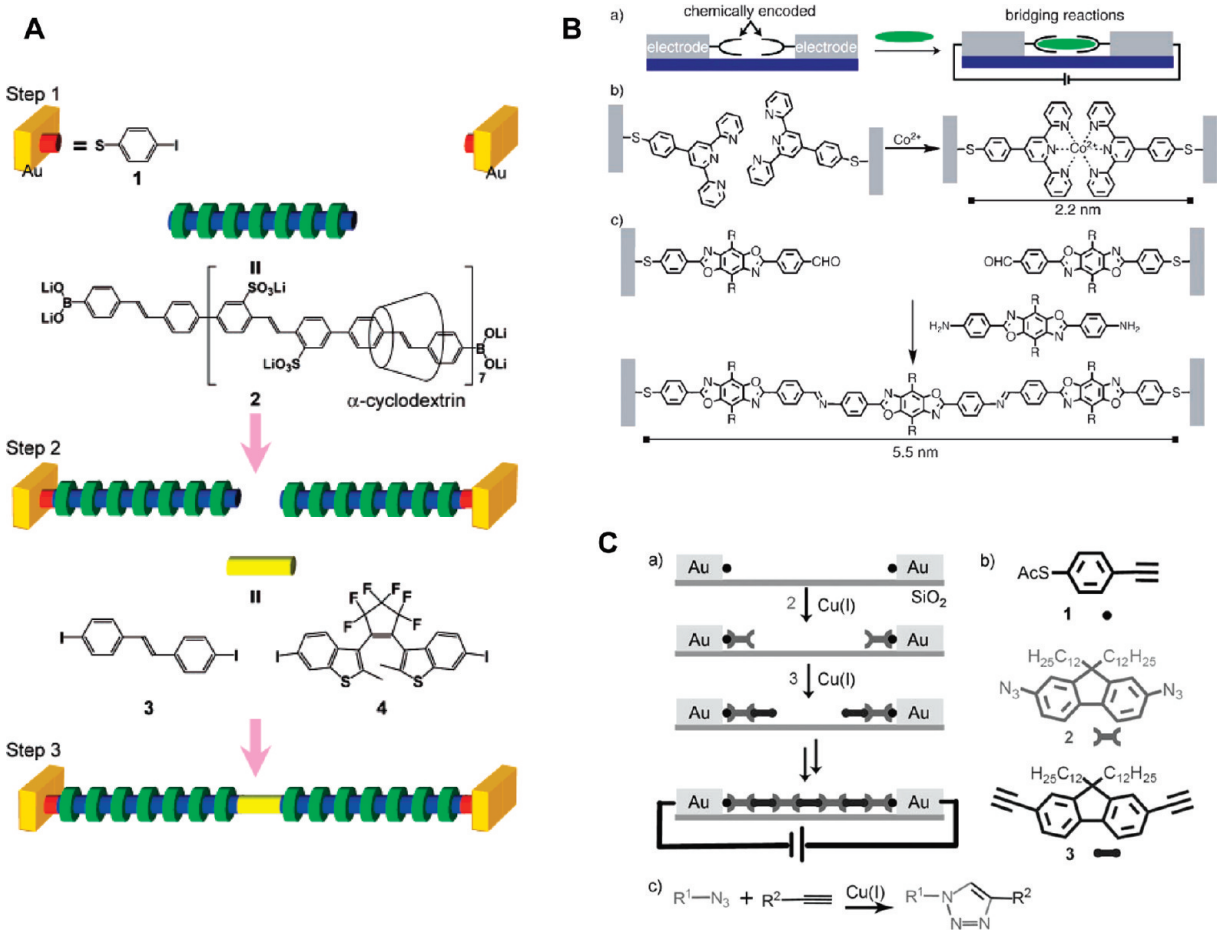

Figure 9. Examples of in situ synthesis of conjugated molecular wires interconnecting closely spaced electrodes. (A) Self-organized interconnect method using Suzuki coupling reactions. Reproduced with permission from ref 73. Copyright 2006 American Chemical Society. (B) Bridging functionalized electrodes with metal coordination and imine formation. Reproduced with permission from ref 74. Copyright 2007 Wiley-VCH Verlag GmbH & Co. KgaA. (C) OWL method to bridge the nanogaps by stepwise click chemistry. Reproduced with permission from ref 75. Copyright 2009 Wiley-VCH Verlag GmbH & Co. KgaA.

moderate temperatures, the rate of tunneling is strongly suppressed and instead charge can be injected into frontier orbitals of the wire molecules and is transported by an incoherent hopping mechanism.[14,104] The transport is generally thermally activated and the length dependence of resistance is predicted to be linear.[14,104−106] Figure 11 is a scheme showing the multistep hopping regime in terms of the molecular energy levels and the electron transport.

For the purposes of this review article, it is convenient to compare the expressions for the low bias junction resistance for tunneling versus thermally assisted hopping mechanisms. For tunneling

$$R = R_0 \exp(\beta L) \qquad (1)$$

where R_0 is the effective contact resistance, L is the molecular length, and $\beta = 2(2m\varphi)^{1/2}/\hbar$ is a structure-dependent tunneling attenuation factor that depends on the effective tunneling barrier height φ, the electron effective mass m, and Planck's constant. The tunneling barrier height φ is often approximated as the energy difference between the Fermi level, E_F, and the closest frontier orbital, e.g., E_{HOMO}. For hopping, the junction resistance follows,

$$R = R_0 + \alpha L = R_0 + \alpha_\infty L \exp\left(\frac{E_a}{kT}\right) \qquad (2)$$

where again R_0 is the contact resistance, $\alpha = \alpha_\infty \exp\left(\frac{E_a}{kT}\right)$ is a molecule specific parameter with units resistance per unit length, L is the molecular length as above, and E_a is the activation energy associated with hopping. One can see from eqs 1 and 2 that tunneling in general has much stronger length dependence than hopping (for typical β values 0.1−1 Å^{-1}). Furthermore, as noted already, strong temperature dependence is very characteristic for hopping, while in tunneling the temperature dependence is weak. The Arrhenius-type thermal activation for hopping transport is readily explained in the Marcus picture of electron transfer.[51,57,107] Thermal motion of nuclei within the molecular wire (e.g., bond rotation and stretching) results in a favorable geometry that facilitates electronic coupling and migration of charge. The activation energy (E_a) corresponds to the energy required to reach the transition state for electron transfer within the wire molecule.

From eqs 1 and 2, we can also observe that a single measurement of low bias junction resistance for a given molecular junction leaves open the question of the relative role of R_0 and the question of transport mechanism (e.g., does eq 1 or 2 apply?). In two-terminal molecular junction measurements, the best way to determine the magnitude of R_0 and thus the values of β (in the tunneling regime) or α (in the hopping regime) is to measure R as a

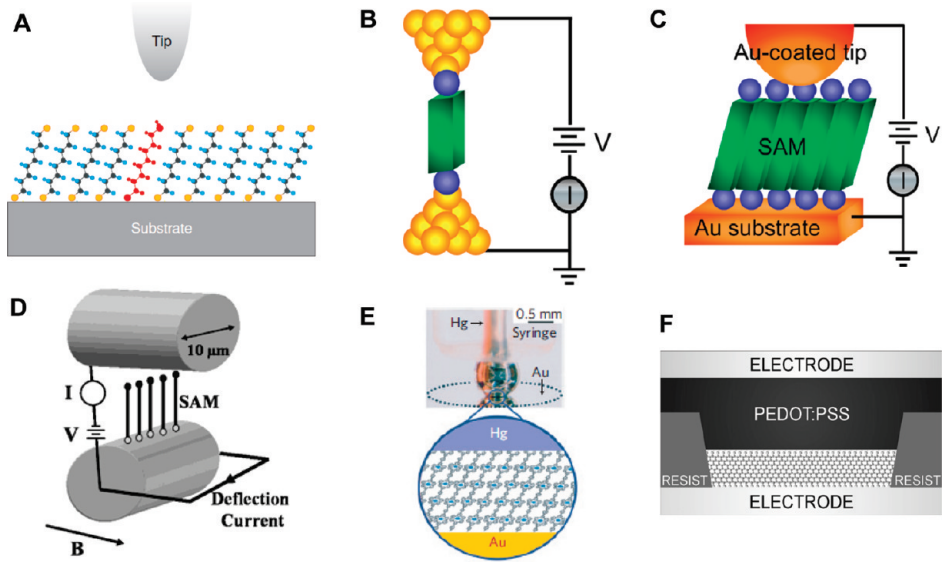

Figure 10. Representative examples of formed metal/wire/metal junctions formed by (A) scanning tunneling microscopy (STM); (B) break junction; (C) CP-AFM; (D) crossed-wire junction; (E) mercury drop junction; (F) conducting polymer top contact. Graphics A and B reproduced with permission from ref 4. Copyright 2007 Annual Reviews. Graphic C reproduced with permission from ref 37. Copyright 2010 American Chemical Society. Graphic D reproduced with permission from ref 95. Copyright 2002 American Chemical Society. Graphic E reproduced with permission from ref 34. Copyright 2009 Nature Publishing Group. Graphic F reproduced with permission from ref 102. Copyright 2008 Institute of Physics.

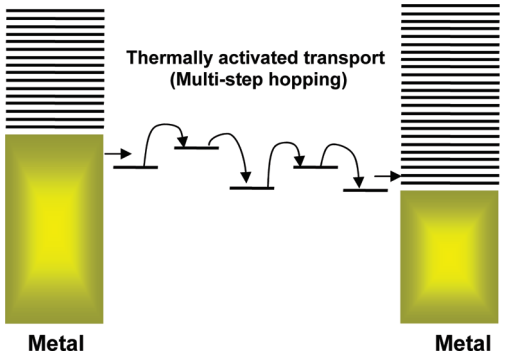

Figure 11. Schematic energy diagram for multistep hopping through a molecular wire between metal electrodes.

function of L. The R versus L data then also indicate the transport mechanism, i.e., if the dependence on L is exponential the mechanism is likely tunneling and if it is linear it is likely hopping. Additionally, the temperature dependence of R is taken to be an excellent indication of transport mechanism.

It is evident from eq 1 that R_0 has a major impact on the total R in the tunneling regime. For example, for two different junctions composed of the same molecules but with R_0 values differing by a factor of 10 (e.g., due to different contacts), total R values will also differ by a factor of 10 because R_0 is a coefficient to the exponential length dependence. However, in the hopping regime, the influence of the contacts is increasingly diminished as L increases because R_0 is an additive term to the L dependence. That is, for very large L, $R \gg R_0$ and so R_0 can be ignored. Thus, junctions made of the same very long wires but with different contact properties will not necessarily exhibit measurably different R values. The point is that the impact of R_0 on tunneling junctions can be much greater than in the hopping regime.

For all molecular junctions, the total resistance R is also a function of the applied bias V across the junction; that is, R is in general a function of V and this dependence can also be diagnostic for transport mechanism changes within a junction. In the following paragraphs, we consider individually the length, temperature, and bias dependence of conduction for both the tunneling and the hopping regimes. Specifically, we recap results in the literature that indicate a transition from tunneling to hopping transport as molecular wire length increases.

4.2. Length-Dependent Conductance. Although the importance of length-dependent molecular wire measurements is recognized, there are very few measurements in the literature that examine length dependent conduction for molecules in the hopping regime ($\gtrsim$ 4 nm). For example, the length dependent measurements of oligophenyleneimine (OPI) wires indicated a transition in transport mechanism from direct tunneling to long-range hopping.[27] Figure 12 shows a semilog plot of resistance versus molecular length for OPI wires, where the resistance was determined using Au-coated CP-AFM tips in contact with the OPI wires grown on Au. Significantly, a clear transition of the length dependence of low voltage resistance was observed near 4 nm (OPI 5), indicating that the conduction mechanism is different in short (OPI 1−5) and long OPI wires (OPI 6−10). In short wires, the exponentially increased resistances indicated that the data were well described by eq 1 for nonresonance tunneling. The β value was found to be 0.3 $Å^{-1}$, which is within the range of β values of typical conjugated molecules. For long OPI wires, a much flatter resistance versus molecular length relation ($\beta \approx 0.09$ $Å^{-1}$) was exhibited, suggesting that the principal transport mechanism is hopping. In addition, the linear plot of R versus L for long wires (Figure 12 inset) was expected for

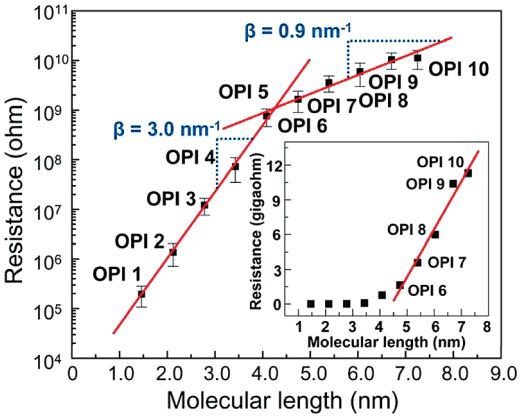

Figure 12. Semilog plot of resistance of OPI wires versus length. Inset: linear plot. Adapted with permission from ref 27. Copyright 2008 the American Association for the Advancement of Science.

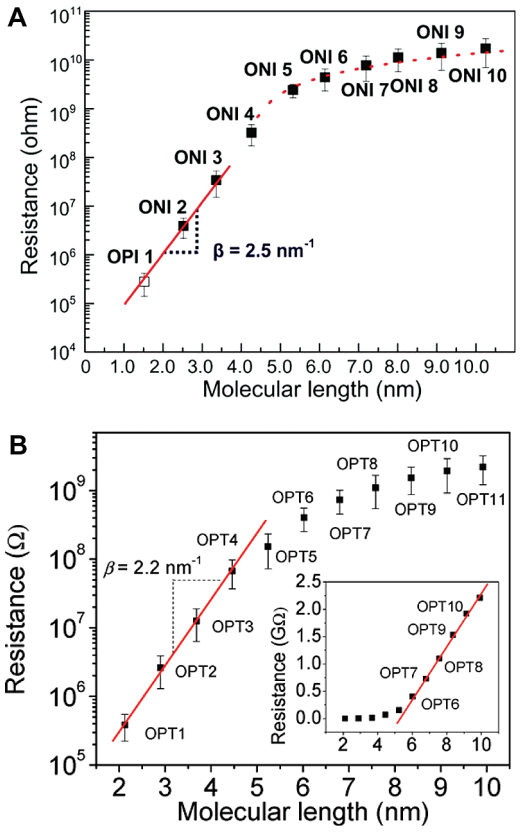

Figure 13. (A) Semiplot of R versus L for the Au/ONI/Au junctions. Reprinted with permission from ref 36. Copyright 2010 the American Chemical Society. (B) Semiplot of R versus L for the Au/OPT/Au junctions. The inset is a linear plot of R versus L according to eq 2. Reproduced with permission from ref 37. Copyright 2010 the American Chemical Society.

hopping transport and indicated that eq 2 applied for the long wires.

The same transition from tunneling to hopping was also observed in the length dependent conduction measurements of oligonaphthalenefluoreneimine (ONI)[36] and oligophenylenetriazole (OPT)[37] wires, as shown in Figure 13. For long ONI wires (ONI 4−10, structures shown in Figure 6(top)), indicated by the dashed line in Figure 13A, the resistances have much weaker length dependence than those for short molecules, as expected

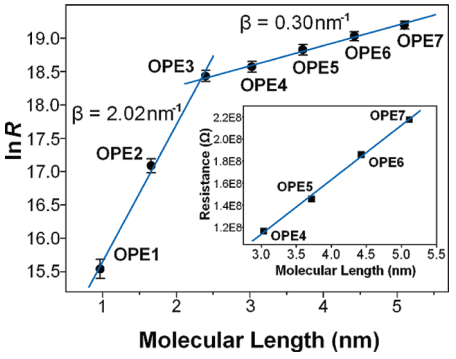

Figure 14. Semilog plot of single molecule resistance against molecular length for all Au/OPE/Au junctions. The inset is a linear plot of R versus L. Reproduced with permission from ref 31. Copyright 2009 the American Chemical Society.

for hopping transport. Based on an estimated number of wires in the junction (~100), a single-wire conductivity of 1×10^{-4} S/cm was calculated from a linear fit of R versus L in the long wire regime (it can be shown that the slope $\alpha = (\sigma A)^{-1}$, where σ is the conductivity and A is the area of the junction). Similarly, the linear relationship of the resistance of long OPT wires (OPT 6−11, Figure 7A) suggests that hopping transport prevails in this regime, Figure 13B inset.

Wang and co-workers have examined the length-dependent conduction of OPE wires ranging from 0.98 to 5.11 nm (shown in Figure 3B) by STM break junction.[31] As exhibited in Figure 14, the β value calculated on the basis of a semilog plot of R versus L for OPE 1−3 was 2.02 nm^{-1}, whereas that for OPE 4−7 was much lower (0.30 nm^{-1}), indicating that a transition occurred between OPE 3 and OPE 4 (near 2.75 nm). The linear characteristic of R against L for long OPE wires fit well with eq 2 (Figure 14 inset), indicating that hopping transport is dominant in this regime.

The transition from tunneling to hopping was also observed in the length dependent resistance measurement of single oligothiophene molecular wires, as shown in Figure 15.[35] Using STM break junctions, Tada and colleagues obtained the electrical resistances of oligothiophene wires (depicted in Figure 3A) ranging from 2.2 nm (5-mer) to 9 nm (23-mer). An exponential increase in the resistance was found for oligothiophenes shorter than the 11-mer, as is typical for tunneling transport (Figure 15A). In contrast, a linear relationship between the molecular length and resistance was observed for molecules longer than the 11-mer, as expected for hopping transport (Figure 15B).

Length dependent measurements were performed on even longer molecular wires in the hopping regime. Rampi et al. have reported the electrical measurements of metal-incorporated nanowires up to 40 nm in length (Figure 16).[34] Although the authors employed β to characterize the length dependent conduction, the obtained extremely low β values of 0.028 $Å^{-1}$ (Fe(II) MWs) and 0.001 $Å^{-1}$ (Co(II) MWs) implicated a multistep charge hopping process between the metal centers in the backbone.

4.3. Temperature Dependence. As noted earlier, thermally activated transport is often an indication of hopping transport. Consequently, here we focus on prior work that

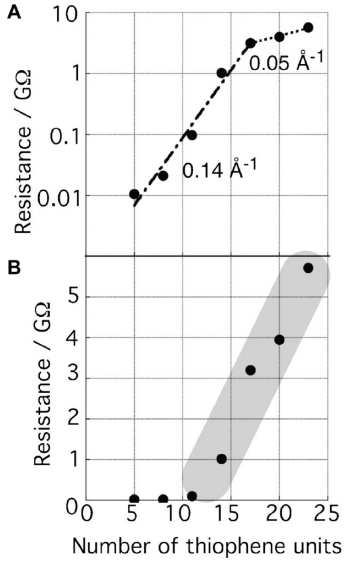

Figure 15. (A) Semilog and (B) linear plots of the resistance as a function of the number of thiophene units. Reproduced with permission from ref 35. Copyright 2009 the Japan Society of Applied Physics.

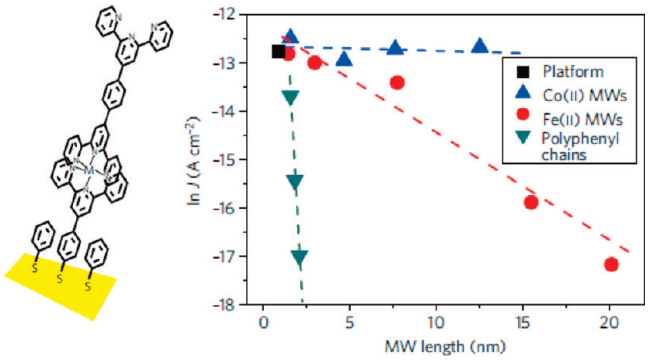

Figure 16. Length-dependent conduction of metal-incorporated nanowires. Reproduced with permission from ref 34. Copyright 2009 Nature Publishing Group.

has shown activated behavior, although carrier hopping within the wires was not always implicated by the authors, and may not be operative, in all of the following examples.

Experimental studies of thermal effects on DC conduction through conjugated molecular wires have been reported in pioneering work on nitro-substituted oligophenylene-ethynylene (OPE) by Selzer et al.[21,22,108] following substantial theoretical efforts.[105,106,109] Figure 17 shows Arrhenius plots of current versus inverse temperature for a single molecule junction in which there is a characteristic transition from temperature-independent behavior at low temperatures, where conduction is dominated by tunneling, to temperature-dependent hopping behavior at high temperatures. The activation energy in the hopping regime corresponds very well with theoretical calculations of barriers for rotations of the rings in the nitro-substituted OPE.[21] The authors proposed that the onset of torsional fluctuation of the phenyl rings leads to vibronic coupling, which suppresses tunneling and facilitates a hopping process. On the contrary, current in the ensemble junction displays temperature independence over the entire temperature range without a transition

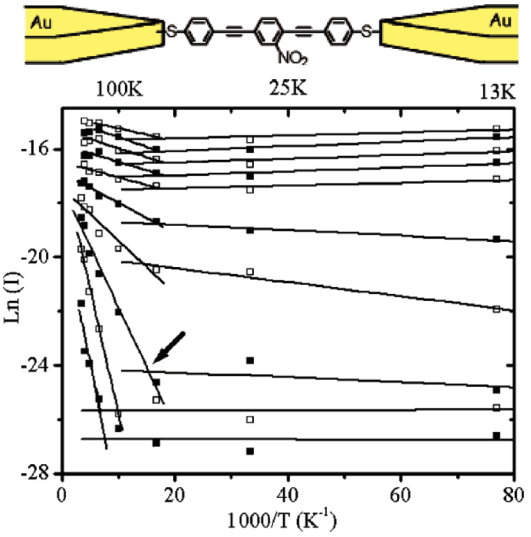

Figure 17. Temperature dependence of the current through 1-nitro-2, 5-di(phenyl-ethynyl-4′-mercapto) benzene wire between Au electrodes, showing transition from nonactivated to activated behavior with a bias-dependent activation energy. The bias increment between plots is 0.1 V, and the bias of the lowest curve is 0.1 V. The transition temperatures are marked by the intersection between lines; see, for example, the arrow for 0.3 V. Adapted with permission from ref 21. Copyright 2004 the American Chemical Society.

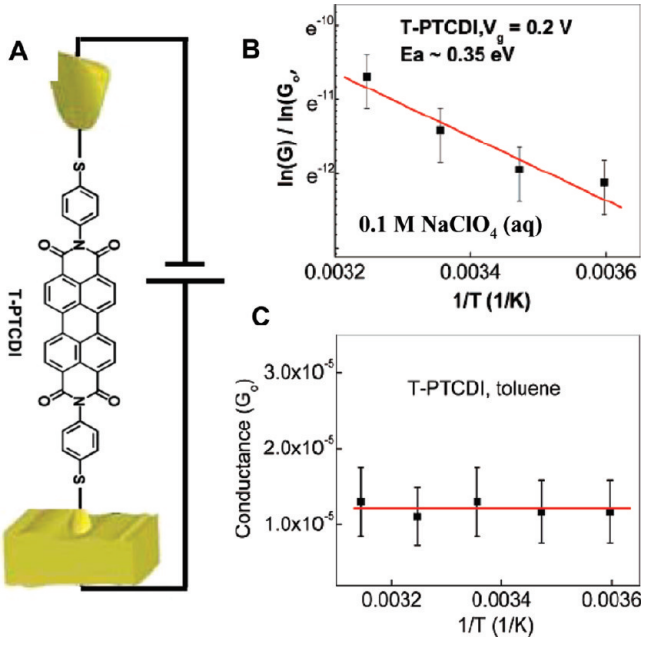

Figure 18. (A) Schematics of T-PTCDI in a STM break junction. Solvent (not shown) surrounds the molecule. (B) Arrhenius plot of conductance versus inverse temperature for T-PTCDI that has been electrochemically reduced in electrolytes. (C) Semilog plot of conductance versus inverse temperature for a T-PTCDI molecule in nonpolar solvent. Adapted with permission from ref 42. Copyright 2007 American Chemical Society.

to hopping (not shown), which the authors suggested is due to a restricted volume for torsional modes in a close packed SAM matrix.[108]

Tao and colleagues[42] have observed thermally activated hopping in redox active perylene tetracarboxylic dimide (PTCDI) molecules connected between an STM tip and a gold substrate with an electrochemical gate, as demonstrated in Figure 18. In these experiments,

charge was electrochemically induced on the PTCDI molecules and conduction through the charged molecules was thermally activated, consistent with a hopping mechanism (Figure 18B). However, when the same molecules were probed without inducing charge, the temperature dependence of conduction was much weaker, indicative of a tunneling mechanism (Figure 18C).

Mirkin et al.[26] studied the temperature dependent $I-V$ characteristics of a 3 nm long OPE-bridged junction (Figure 19) to elucidate the conduction mechanism of the

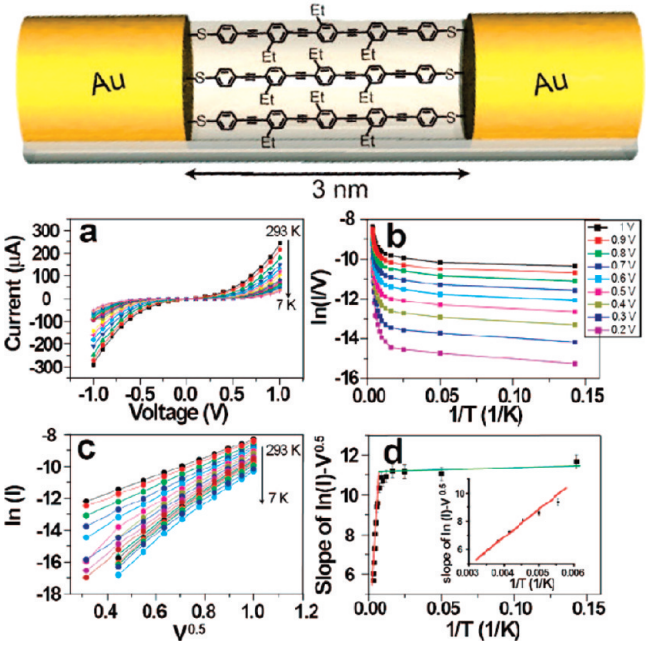

Figure 19. a) Temperature dependent $I-V$ response of the OPE bridged nanogap junction on top. (b) Plots of $\ln(I/V)$ as a function of $1/T$ for different biases. (c) Plots of $\ln(I)$ vs $V^{0.5}$ with biases from 0.1 to 1.0 V at different temperature. (d) Plot of the slop of $\ln(I)-V^{0.5}$ vs $1/T$. The inset shows the magnification of the high-temperature part with linear fitting. All of the straight lines are χ^2 fits for respective data sets. Reproduced from ref 26. Copyright 2008 the American Chemical Society.

device, and observed a transition from tunneling to thermally activated transport when temperature increases. At low temperatures (<120 K), charge transport was dominated by direct tunneling, where the $I-V$ response was minimally dependent upon temperature. At higher temperature, the current of the junction increased with temperature (Figure 19a), suggesting a thermally activated transport mechanism. A thermionic emission mechanism was proposed based on the observation of the linear relationship between $\ln(I)$ and $V^{0.5}$ (Figure 19c).[110,111] The plot of (I/V) versus $1/T$ exhibited a clear difference as a function of voltage (Figure 19b), which the authors interpreted as inconsistent with a hopping mechanism. Alternatively, it is possible that the mechanism is hopping with a bias-dependent charge mobility.

Temperature-dependent CP-AFM measurements on short (OPI 4 and 5) and long (OPI 6 and 10) conjugated wires were performed by Choi and co-workers and are summarized as an Arrhenius plot of resistance versus $1/T$ in Figure 20.[27] Clearly, the resistances for OPI 4 and OPI 5 are independent of temperature from 246 to 333 K, as expected for tunneling. However, both OPI 6 and OPI 10 displayed strongly thermally activated transport characteristic of hopping. The activation energies determined from the slopes of the data were identical at 0.64 eV (15.0 kcal/mol) for both OPI 6 and 10, which implied that the same molecular motion contributes to the intramolecular hopping process in both wires. Collectively, the data in both length and temperature-dependent resistance measurements provide unambiguous evidence for a mechanistic transition from tunneling to hopping near 4 nm in OPI wire length.

Choi et al. have also measured temperature dependent resistance for ONI wires to better understand the nature of the charge carriers and the hopping process (Figure 21).[36] As illustrated in Figure 21A, the resistance for ONI 3 was independent of temperature from 246 to 333 K, but the resistance for ONI 4 was strongly

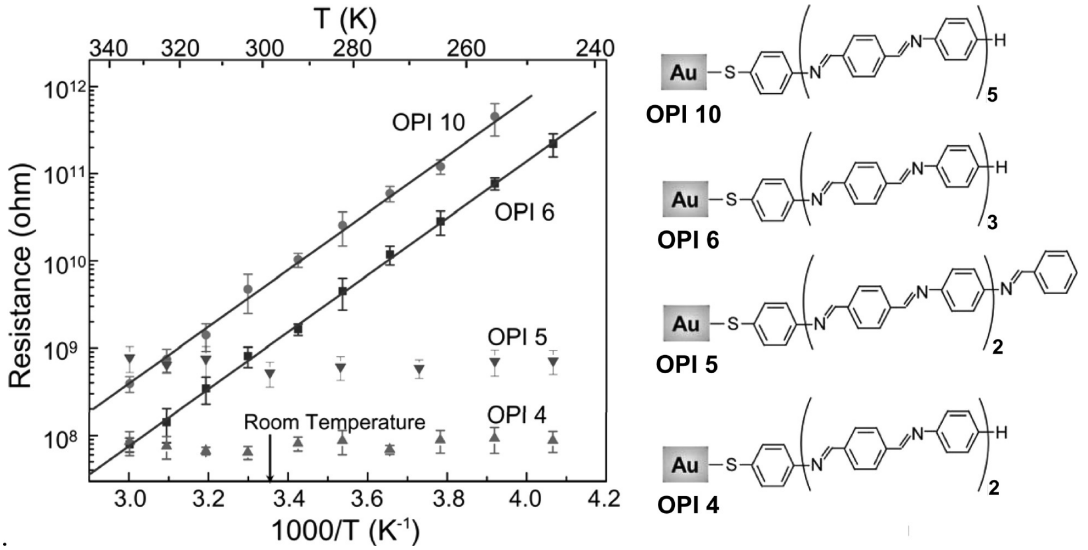

Figure 20. Arrhenius plots for resistance versus temperature data for short (OPI 4 and OPI 5) and long wires (OPI 6 and OPI 10). Adapted with permission from ref 27. Copyright 2008 the American Association for the Advancement of Science.

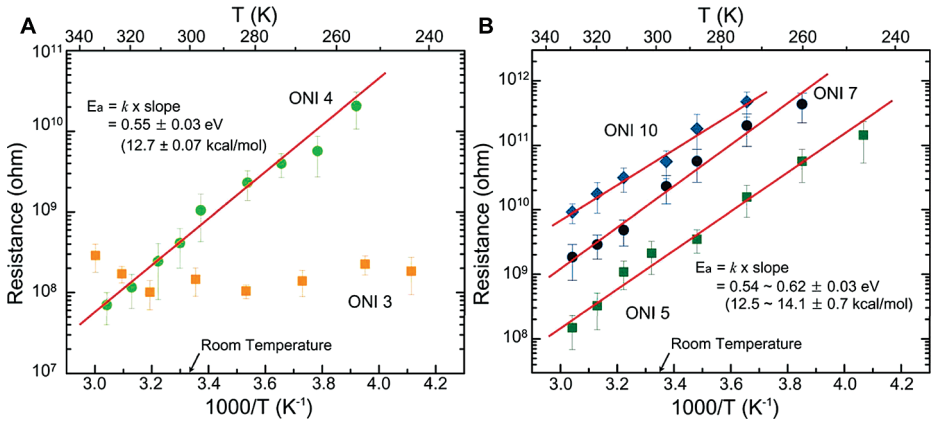

Figure 21. Arrhenius plot for (A) ONI 3 and ONI 4 and (B) ONI 5, ONI 7, and ONI 10. Straight lines are linear fits to the data. Reproduced with permission from ref 36. Copyright 2010 the American Chemical Society.

thermally activated, consistent with their respective transport mechanisms inferred from length dependent conduction. The nearly identical activation energies E_a for long wires (Figure 21B) implied the same rate-determining step for hopping transport regardless of the wire length. The E_a determined from the slopes in Figure 21B (0.54−0.62 eV) was a factor of 2−3 higher than those obtained from quantum chemical calculations (~0.2 eV), possibly because molecular relaxation energies of the ONI molecules in a SAM may be significantly greater than isolated molecules, and in turn impact reorganization energies upon charge transfer.[108] Very recent studies on charge transport characteristics of ensemble carbon/azobenzene/Cu junctions observed very weak temperature dependence.[112] The apparent E_a of 0.1 eV was too small to implicate solid-state nuclear motion, but could be attributed to the broadened Fermi function in the contacts at higher temperature. Clearly, carefully determining the nature and origin of the activation energy for transport processes is of great interest.

4.4. Voltage Dependence. The transport results discussed so far were obtained predominantly at low junction biases. Indeed, at voltages below 0.1 V, most molecular junctions exhibit ohmic behavior (i.e., $I = V/R$). However, to have a complete understanding of transport in a molecular wire, it is necessary to characterize the voltage and electric field dependence of the $I-V$ characteristics.[113] Applying increased bias across a junction may perturb the electronic structure of the wire, as the electric fields may be as large as 1×10^5 to 1×10^7 V/cm, but also in the hopping regime additional carriers may be injected into the wires. There can be field driven changes in conduction mechanisms.

Currently, however, there is very little data in the literature concerning the bias dependence of transport in long conjugated molecules, particularly those in which hopping transport dominates. One exception is the work by Choi, et al.[27,36] Figure 22 shows log−log $I-V$ plots for two different ONI wire assemblies, one based on short ONI 3 molecules (tunneling wires) and the other based on longer ONI 8 molecules (hopping wires). It is clear from the different voltage domains that both wire molecules exhibit

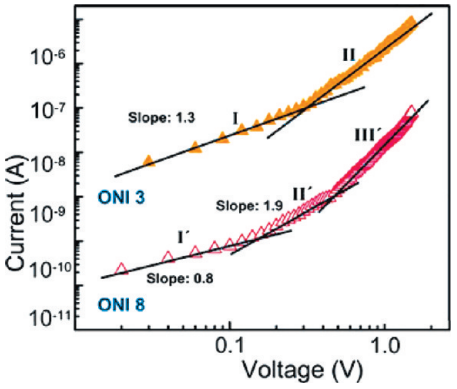

Figure 22. Log−log plot of the $I-V$ curves for typical short and long ONI molecular wires. Adapted with permission from ref 36. Copyright 2010 the American Chemical Society.

changes in transport behavior as the junction bias increases. Specifically, it appears that a power law applies, i.e., $I \propto V^n$, where n systematically changes in the different domains.

At the present time, the origin of the different domains is still not clear. At low voltages both short (ONI 3) and long (ONI 8) exhibit approximately ohmic behavior. This is expected because for both tunneling and hopping one predicts $I \propto V$ at least at low voltage. ONI 3 exhibits a change to steeper dependence of I on V (higher n) at ~0.3 V which has been attributed potentially to the onset of field-assisted tunneling. ONI 8, on the other hand, has perhaps three different transport regimes over the 0−1 V bias range. A possible explanation is a transition from ohmic to space-charge-limited conduction (SCLC) in which additional charge carriers (probably holes in the case of ONI between Au electrodes) are injected into the wire backbones and the current is dominated by the drift component of the injected carriers. Classically, the space-charge-limited current is given by the Mott−Gurney Law[114]

$$J = \frac{9\varepsilon\mu V^2}{8L^3} \text{ or } I \propto V^2 \qquad (3)$$

where ε is the dielectric constant, μ is the charge mobility, and L is the wire length. The slope of 1.9 in the log I versus

log V plot of ONI 8 (Figure 22) is consistent with an SCLC transport mechanism in this voltage range. In addition, if charge traps are present in a conductor, the slope can vary greatly. Thus, higher power domains may correspond to a transition to trap-limited SCLC behavior, for example. But there are other factors that might be involved as well, such as field-dependent carrier mobilities. The bias dependence of transport for hopping wires is likely to be quite complex, and more systematic measurements, for example as a function of intentional wire doping, will be necessary to elucidate the different transport domains.

5. Future Prospects

As discussed in this short review, the ability to examine multistep hopping conduction in ensembles of molecular wires has been made possible by a combination of new molecular synthesis approaches with reproducible and convenient molecular junction testbeds. However, study of hopping transport in molecular junctions is currently in a very early stage and in considering the future prospects of this research area, it is reasonable to ask what can be learned, what are the key unanswered questions, and what it likely to be different about the hopping regime from the more well-studied tunneling regime.

In terms of new knowledge, the ability to measure DC hopping conduction in wires with precisely controlled lengths and architectures presents exciting opportunities to explore the physical organic chemistry of hopping transport. New molecules can be made with control over intramolecular bond torsion angles (planarity), conjugation length, and electronic structure, for example, and their resistances (conductivities) can be directly compared. HOMO and LUMO levels can also be systematically shifted by judicious choice of side groups to examine and compare electron conduction versus hole conduction. And conjugation can be intentionally disrupted or blocked by insertion of saturated building blocks to address the role of chain defects on through-wire hopping. Well-defined redox-centers can also be incorporated into wires, which might allow observation of interesting charge (electron−electron or hole−hole) correlation effects. These systematic structure−property correlations promise to dramatically enhance our understanding of conduction in molecular systems.

There are of course currently many unanswered questions. In most of the examples cited in this review, the number or concentration of charge carriers per wire is essentially unknown and uncontrolled. Indeed, even the mechanism by which the carriers are introduced into the wires is unclear. Knowledge of carrier concentration is essential for determining the hole or electron mobility, i.e., the average speed of the carrier per unit electric field, which in turn should be directly related to the bonding architecture of the wire molecules. In addition, it is not so clear currently how to picture the carriers on molecular wires- if the carriers form polarons, for example, how localized or delocalized are the polarons, and what is the polaron "binding energy" and what relation does that have to the measured transport activation energy? Of course, there is also the open question for wire ensembles of the role of interwire interactions, namely to what extent is the ensemble functioning as a collection of independent, parallel wires versus a tightly coupled cluster? Clearly, these kinds of questions are challenging and will require many carefully designed experiments to address.

Finally, it is certainly reasonable to consider how the spectrum of molecular junction transport behavior will be different for hopping versus tunneling conduction and whether there are any advantages of hopping for potential molecular electronics applications. For example, in hopping conduction is it possible to have more control over the junction $I-V$ characteristics? In the hopping regime, can we find more simple and rational design principles to obtain, for instance, current rectification or bistable conductance at room temperature? Are contact effects essentially always dominating in tunnel junctions and less so in hopping junctions? How does heat dissipation factor in hopping versus tunneling junctions? Clearly, many more experiments are necessary to adequately address these issues. However, at this point, it seems evident that the systematic examination of hopping conduction in molecular wires will be an exciting new research area for chemists and physicists.

Acknowledgment. Portions of the work described here were supported primarily by the National Science Foundation under CHE-0616427. Partial support for facilities was provided by the NSF MRSEC program under Award DMR-0819885.

References

(1) Salomon, A.; Cahen, D.; Lindsay, S.; Tomfohr, J.; Engelkes, V. B.; Frisbie, C. D. *Adv. Mater.* **2003**, *15*, 1881–1890.
(2) McCreery, R. L. *Chem. Mater.* **2004**, *16*, 4477–4496.
(3) Selzer, Y.; Allara, D. L. *Annu. Rev. Phys. Chem.* **2006**, *57*, 593–623.
(4) Chen, F.; Hihath, J.; Huang, Z. F.; Li, X. L.; Tao, N. J. *Annu. Rev. Phys. Chem.* **2007**, *58*, 535–564.
(5) McCreery, R. L.; Bergren, A. J. *Adv. Mater.* **2009**, *21*, 4303–4322.
(6) Kim, Y.; Cook, S.; Tuladhar, S. M.; Choulis, S. A.; Nelson, J.; Durrant, J. R.; Bradley, D. D. C.; Giles, M.; McCulloch, I.; Ha, C. S.; Ree, M. *Nat. Mater.* **2006**, *5*, 197–203.
(7) Peet, J.; Kim, J. Y.; Coates, N. E.; Ma, W. L.; Moses, D.; Heeger, A. J.; Bazan, G. C. *Nat. Mater.* **2007**, *6*, 497–500.
(8) Sirringhaus, H.; Tessler, N.; Friend, R. H. *Science* **1998**, *280*, 1741–1744.
(9) Shen, Z. L.; Burrows, P. E.; Bulovic, V.; Forrest, S. R.; Thompson, M. E. *Science* **1997**, *276*, 2009–2011.
(10) Yan, H.; Chen, Z. H.; Zheng, Y.; Newman, C.; Quinn, J. R.; Dotz, F.; Kastler, M.; Facchetti, A. *Nature* **2009**, *457*, 679–U1.
(11) Cho, J. H.; Lee, J.; Xia, Y.; Kim, B.; He, Y. Y.; Renn, M. J.; Lodge, T. P.; Frisbie, C. D. *Nat. Mater.* **2008**, *7*, 900–906.
(12) Heath, J. R.; Ratner, M. A. Phys. Today **2003**, May 43−49.
(13) Nitzan, A.; Ratner, M. A. *Science* **2003**, *300*, 1384–1389.
(14) Joachim, C.; Ratner, M. A. *Proc. Natl. Acad. Sci. U.S.A.* **2005**, *102*, 8801–8808.
(15) Joachim, C.; Gimzewski, J. K.; Aviram, A. *Nature* **2000**, *408*, 541–548.
(16) Kwok, K. S.; Ellenbogen, J. C. Mater. Today **2002**, Feb, 28−37.
(17) Tao, N. J. *Nat. Nanotechnol.* **2006**, *1*, 173–181.
(18) Park, J.; Pasupathy, A. N.; Goldsmith, J. I.; Chang, C.; Yaish, Y.; Petta, J. R.; Rinkoski, M.; Sethna, J. P.; Abruna, H. D.; McEuen, P. L.; Ralph, D. C. *Nature* **2002**, *417*, 722–725.
(19) Kubatkin, S.; Danilov, A.; Hjort, M.; Cornil, J.; Bredas, J.-L.; Stuhr-Hansen, N.; Hedegard, P.; Bjornholm, T. *Nature* **2003**, *425*, 698–701.
(20) Fan, F. R. F.; Yang, J. P.; Cai, L. T.; Price, D. W.; Dirk, S. M.; Kosynkin, D. V.; Yao, Y. X.; Rawlett, A. M.; Tour, J. M.; Bard, A. J. *J. Am. Chem. Soc.* **2002**, *124*, 5550–5560.
(21) Selzer, Y.; Cabassi, M. A.; Mayer, T. S.; Allara, D. L. *J. Am. Chem. Soc.* **2004**, *126*, 4052–4053.

(22) Selzer, Y.; Cabassl, M. A.; Mayer, T. S.; Allara, D. L. *Nanotechnology* **2004**, *15*, S483–S488.
(23) Kang, B. K.; Aratani, N.; Lim, J. K.; Kim, D.; Osuka, A.; Yoo, K. H. *Chem. Phys. Lett*. **2005**, *412*, 303–306.
(24) Tran, E.; Grave, C.; Whitesides, G. A.; Rampi, M. A. *Electrochim. Acta* **2005**, *50*, 4850–4856.
(25) Troisi, A.; Ratner, M. A. *Small* **2006**, *2*, 172–181.
(26) Chen, X.; Jeon, Y. M.; Jang, J. W.; Qin, L.; Huo, F.; Wei, W.; Mirkin, C. A. *J. Am. Chem. Soc*. **2008**, *130*, 8166–8168.
(27) Choi, S. H.; Kim, B.; Frisbie, C. D. *Science* **2008**, *320*, 1482–1486.
(28) Seitz, O.; Vilan, A.; Cohen, H.; Hwang, J.; Haeming, M.; Schoell, A.; Umbach, E.; Kahn, A.; Cahen, D. *Adv. Funct. Mater*. **2008**, *18*, 2102–2113.
(29) Nozaki, D.; Girard, Y.; Yoshizawa, K. *J. Phys. Chem. C* **2008**, *112*, 17408–17415.
(30) DiBenedetto, S. A.; Facchetti, A.; Ratner, M. A.; Marks, T. J. *J. Am. Chem. Soc*. **2009**, *131*, 7158–7168.
(31) Lu, Q.; Liu, K.; Zhang, H. M.; Du, Z. B.; Wang, X. H.; Wang, F. S. *ACS Nano* **2009**, *3*, 3861–3868.
(32) McCreery, R. L. *ChemPhysChem* **2009**, *10*, 2387–2391.
(33) Okamoto, S.; Morita, T.; Kimura, S. *Langmuir* **2009**, *25*, 3297–3304.
(34) Tuccitto, N.; Ferri, V.; Cavazzini, M.; Quici, S.; Zhavnerko, G.; Licciardello, A.; Rampi, M. A. *Nat. Mater*. **2009**, *8*, 41–46.
(35) Yamada, R.; Kumazawa, H.; Tanaka, S.; Tada, H. *Appl. Phys. Express* **2009**, *2*, 3.
(36) Choi, S. H.; Risko, C.; Ruiz Delgado, M. C.; Kim, B.; Bredas, J.-L.; Frisbie, C. D. *J. Am. Chem. Soc*. **2010**, *132*, 4358–4368.
(37) Luo, L.; Frisbie, C. D. *J. Am. Chem. Soc*. **2010**, *132*, 8854–8855.
(38) Simeone, F. C.; Rampi, M. A. *Chimia* **2010**, *64*, 362–369.
(39) Sedghi, G.; Sawada, K.; Esdaile, L. J.; Hoffmann, M.; Anderson, H. L.; Bethell, D.; Haiss, W.; Higgins, S. J.; Nichols, R. J. *J. Am. Chem. Soc*. **2008**, *130*, 8582–8583.
(40) Yamada, R.; Kumazawa, H.; Noutoshi, T.; Tanaka, S.; Tada, H. *Nano Lett*. **2008**, *8*, 1237–1240.
(41) Xing, Y. J.; Park, T. H.; Venkatramani, R.; Keinan, S.; Beratan, D. N.; Therien, M. J.; Borguet, E. *J. Am. Chem. Soc*. **2010**, *132*, 7946–7956.
(42) Li, X.; Hihath, J.; Chen, F.; Masuda, T.; Zang, L.; Tao, N. J. *J. Am. Chem. Soc*. **2007**, *129*, 11535–11542.
(43) Choi, S. H.; Frisbie, C. D. *J. Am. Chem. Soc*. **2010**, in press.
(44) Ulgut, B.; Abruna, H. D. *Chem. Rev*. **2008**, *108*, 2721–2736.
(45) Moth-Poulsen, K.; Bjornholm, T. *Nat. Nanotechnol*. **2009**, *4*, 551–556.
(46) Zhang, J. D.; Kuznetsov, A. M.; Medvedev, I. G.; Chi, Q. J.; Albrecht, T.; Jensen, P. S.; Ulstrup, J. *Chem. Rev*. **2008**, *108*, 2737–2791.
(47) Chen, F.; Tao, N. J. *Acc. Chem. Res*. **2009**, *42*, 429–438.
(48) Lindsay, S. M.; Ratner, M. A. *Adv. Mater*. **2007**, *19*, 23–31.
(49) L.Closs, G.; Miller, J. R. *Science* **1988**, *240*, 440–447.
(50) Jordan, K. D.; Paddon-row, M. N. *Chem. Rev*. **1992**, *92*, 395–410.
(51) Marcus, R. A. *Angew. Chem., Int. Ed*. **1993**, *32*, 1111–1222.
(52) Barbara, P. F.; Meyer, T. J.; Ratner, M. A. *J. Phys. Chem*. **1996**, *100*, 13148–13168.
(53) Davis, W. B.; Svec, W. A.; Ratner, M. A.; Wasielewski, M. R. *Nature* **1998**, *396*, 60–63.
(54) Weiss, E. A.; Tauber, M. J.; Kelley, R. F.; Ahrens, M. J.; Ratner, M. A.; Wasielewski, M. R. *J. Am. Chem. Soc*. **2005**, *127*, 11842–11850.
(55) Paulson, B.; Pramod, K.; Eaton, P.; Closs, G.; Miller, J. R. *J. Phys. Chem*. **1993**, *97*, 13042–13045.
(56) Lambert, C.; Noll, G.; Schelter, J. *Nat. Mater*. **2002**, *1*, 69–73.
(57) Berlin, Y. A.; Hutchison, G. R.; Rempala, P.; Ratner, M. A.; Michl, J. *J. Phys. Chem. A* **2003**, *107*, 3970–3980.
(58) Marcus, R. A.; Sutin, N. *Biochim. Biophys. Acta* **1985**, *811*, 265–322.
(59) Adams, D. M.; Brus, L.; Chidsey, C. E. D.; Creager, S.; Creutz, C.; Kagan, C. R.; Kamat, P. V.; Lieberman, M.; Lindsay, S.; Marcus, R. A.; Metzger, R. M.; Michel-Beyerle, M. E.; Miller, J. R.; Newton, M. D.; Rolison, D. R.; Sankey, O.; Schanze, K. S.; Yardley, J.; Zhu, X. Y. *J. Phys. Chem. B* **2003**, *107*, 6668–6697.
(60) Zhu, X.-Y. *J. Phys. Chem. B* **2004**, *108*, 8778–8793.
(61) Zhu, X. Y. *Surf. Sci. Rep*. **2004**, *56*, 1–83.
(62) Hu, W. P.; Jiang, J.; Nakashima, H.; Luo, Y.; Kashimura, Y.; Chen, K. Q.; Shuai, Z.; Furukawa, K.; Lu, W.; Liu, Y. Q.; Zhu, D. B.; Torimitsu, K. *Phys. Rev. Lett*. **2006**, *96*, 4.
(63) Ashwell, G. J.; Urasinska, B.; Wang, C. S.; Bryce, M. R.; Grace, I.; Lambert, C. J. *Chem. Commun*. **2006**, 4706–4708.
(64) Hines, T.; Diez-Perez, I.; Hihath, J.; Liu, H. M.; Wang, Z. S.; Zhao, J. W.; Zhou, G.; Muellen, K.; Tao, N. J. *J. Am. Chem. Soc*. **2010**, *132*, 11658–11664.
(65) Lafferentz, L.; Ample, F.; Yu, H.; Hecht, S.; Joachim, C.; Grill, L. *Science* **2009**, *323*, 1193–1197.
(66) Rosink, J. J. W. M.; Blauw, M. A.; Geerligs, L. J.; van der Drift, E.; Rousseeuw, B. A. C.; Radelaar, S.; Sloof, W. G.; Fakkeldij, E. J. M. *Langmuir* **2000**, *16*, 4547–4553.
(67) Love, J. C.; Estroff, L. A.; Kriebel, J. K.; Nuzzo, R. G.; Whitesides, G. M. *Chem. Rev*. **2005**, *105*, 1103–1169.
(68) Iha, R. K.; Wooley, K. L.; Nystrom, A. M.; Burke, D. J.; Kade, M. J.; Hawker, C. J. *Chem. Rev*. **2009**, *109*, 5620–5686.
(69) Nebhani, L.; Barner-Kowollik, C. *Adv. Mater*. **2009**, *21*, 3442–3468.
(70) Rostovtsev, V. V.; Green, L. G.; Fokin, V. V.; Sharpless, K. B. *Angew. Chem., Int. Ed*. **2002**, *41*, 2596–2599.
(71) Jiao, J.; Anariba, F.; Tiznado, H.; Schmidt, I.; Lindsey, J. S.; Zaera, F.; Bocian, D. F. *J. Am. Chem. Soc*. **2006**, *128*, 6965–6974.
(72) Lin, C.; Kagan, C. R. *J. Am. Chem. Soc*. **2003**, *125*, 336–337.
(73) Taniguchi, M.; Nojima, Y.; Yokota, K.; Terao, J.; Sato, K.; Kambe, N.; Kawai, T. *J. Am. Chem. Soc*. **2006**, *128*, 15062–15063.
(74) Tang, J.; Wang, Y.; Klare, J. E.; Tulevski, G. S.; Wind, S. J.; Nuckolls, C. *Angew. Chem., Int. Ed*. **2007**, *46*, 3892–3895.
(75) Chen, X. D.; Braunschweig, A. B.; Wiester, M. J.; Yeganeh, S.; Ratner, M. A.; Mirkin, C. A. *Angew. Chem., Int. Ed*. **2009**, *48*, 5178–5181.
(76) Bumm, L. A.; Arnold, J. J.; Cygan, M. T.; Dunbar, T. D.; Burgin, T. P.; Jones, L.; Allara, D. L.; Tour, J. M.; Weiss, P. S. *Science* **1996**, *271*, 1705–1707.
(77) Tao, N. J. *Phys. Rev. Lett*. **1996**, *76*, 4066–4069.
(78) Blum, A. S.; Kushmerick, J. G.; Long, D. P.; Patterson, C. H.; Yang, J. C.; Henderson, J. C.; Tour, J. M.; Shashidhar, R.; Ratna, B. R. *Nat. Mater*. **2005**, *4*, 167–172.
(79) Reed, M. A.; Zhou, C.; Muller, C. J.; Burgin, T. P.; Tour, J. M. *Science* **1997**, *278*, 252–254.
(80) Xu, B.; Tao, N. J. *Science* **2003**, *301*, 1221–1223.
(81) Reichert, J.; Ochs, R. D.; Beckmann, D.; Weber, H. B.; Mayor, M.; L. Closs, G.; von Lohneysen, H. *Phys. Rev. Lett*. **2002**, *88*, 176804.
(82) Venkataraman, L.; Klare, J. E.; Nuckolls, C.; Hybertsen, M. S.; Steigerwald, M. L. *Nature* **2006**, *442*, 904–907.
(83) Beebe, J. M.; Kim, B.-S.; Gadzuk, J. W.; Frisbie, C. D.; Kushmerick, J. G. *Phys. Rev. Lett*. **2006**, *97*, 026801.
(84) Engelkes, V. B.; Beebe, J. M.; Frisbie, C. D. *J. Phys. Chem. B*. **2005**, *106*, 16801–16810.
(85) Wold, D. J.; Haag, R.; Rampi, M. A.; Frisbie, C. D. *J. Phys. Chem. B* **2002**, *106*, 2813–2816.
(86) Beebe, J. M.; Engelkes, V. B.; Miller, L. L.; Frisbie, C. D. *J. Am. Chem. Soc*. **2002**, *124*, 11268–11269.
(87) Kelley, T. W.; Granstrom, E.; Frisbie, C. D. *Adv. Mater*. **1999**, *11*, 261–264.
(88) Wold, D. J.; Frisbie, C. D. *J. Am. Chem. Soc*. **2000**, *122*, 2970–2971.
(89) Kim, B.-S.; Beebe, J. M.; Jun, Y.; Zhu, X. Y.; Frisbie, C. D. *J. Am. Chem. Soc*. **2006**, *128*, 4970–4971.
(90) Wold, D. J.; Frisbie, C. D. *J. Am. Chem. Soc*. **2001**, *123*, 5549–5556.
(91) Cui, X. D.; Primak, A.; Zarate, X.; Tomfohr, J.; Sankey, O. F.; Moore, A. L.; Moore, T. A.; Gust, D.; Harris, G.; Lindsay, S. M. *Science* **2001**, *294*, 571–574.
(92) Leatherman, G.; Durantini, E. N.; Gust, D.; Moore, T. A.; Moore, A. L.; Stone, S.; Zhou, Z.; Rez, P.; Liu, Y. Z.; Lindsay, S. M. *J. Phys. Chem. B* **1999**, *103*, 4006–4010.
(93) Liu, K.; Li, G. R.; Wang, X. H.; Wang, F. S. *J. Phys. Chem. C* **2008**, *112*, 4342–4349.
(94) Engelkes, V. B.; Beebe, J. M.; Frisbie, C. D. *J. Am. Chem. Soc*. **2004**, *126*, 14287–14296.
(95) Kushmerick, J. G.; Holt, D. B.; Pollack, S. K.; Ratner, M. A.; Yang, J. C.; Schull, T. L.; Naciri, J.; Moore, M. H.; Shashidhar, R. *J. Am. Chem. Soc*. **2002**, *124*, 10654.
(96) Kim, B.; Beebe, J. M.; Olivier, C.; Rigaut, S.; Touchard, D.; Kushmerick, J. G.; Zhu, X. Y.; Frisbie, C. D. *J. Phys. Chem. C* **2007**, *111*, 7521–7526.
(97) Anariba, F.; McCreery, R. L. *J. Phys. Chem. B* **2002**, *106*, 10355–10362.
(98) Slowinski, K.; Fong, H. K. Y.; Majda, M. *J. Am. Chem. Soc*. **1999**, *121*, 7257.
(99) Holmlin, R. E.; Haag, R.; Chabinyc, M. L.; Ismagilov, R. F.; Cohen, A. E.; Terfort, A.; Rampi, M. A.; Whitesides, G. M. *J. Am. Chem. Soc*. **2001**, *123*, 5075–5085.
(100) Akkerman, H. B.; Blom, P. W. M.; de Leeuw, D. M.; de Boer, B. *Nature* **2006**, *441*, 69–72.
(101) Van Hal, P. A.; Smits, E. C. P.; Geuns, T. C. T.; Akkerman, H. B.; De Brito, B. C.; Perissinotto, S.; Lanzani, G.; Kronemeijer, A. J.; Geskin, V.; Cornil, J.; Blom, P. W. M.; De Boer, B.; De Leeuw, D. M. *Nat. Nanotechnol*. **2008**, *3*, 749–754.
(102) Akkerman, H. B.; de Boer, B. *J. Phys.: Condens. Matter* **2008**, *20*, 013001.
(103) Bonifas, A. P.; McCreery, R. L. *Nat. Nanotechnol*. **2010**, *5*, 612–617.
(104) Nitzan, A. *Annu. Rev. Phys. Chem*. **2001**, *52*, 681–750.
(105) Segal, D.; Nitzan, A.; Davis, W. B.; Wasielewski, M. R.; Ratner, M. A. *J. Phys. Chem. B* **2000**, *104*, 3817–3829.
(106) Segal, D.; Nitzan, A.; Ratner, M.; Davis, W. B. *J. Phys. Chem. B* **2000**, *104*, 2790–2793.
(107) Zade, S. S.; Bendikov, M. *Chem.—Eur. J*. **2008**, *14*, 6734–6741.
(108) Selzer, Y.; Cai, L.; Cabassi, M. A.; Yao, Y.; Tour, J. M.; Mayer, T. S.; Allara, D. L. *Nano Lett*. **2005**, *5*, 61–65.
(109) Segal, D.; Nitzan, A. *Chem. Phys*. **2001**, *268*, 315–335.
(110) Chen, J.; Calvet, L. C.; Reed, M. A.; Carr, D. W.; Grubisha, D. S.; Bennett, D. W. *Chem. Phys. Lett*. **1999**, *313*, 741.
(111) Wang, W.; Lee, T.; Reed, M. A. *Phys. Rev. B* **2003**, *68*, 035416.
(112) Bergren, A. J.; McCreery, R. L.; Stoyanov, S. R.; Gusarov, S.; Kovalenko, A. *J. Phys. Chem. C* **2010**, *114*, 15806–15815.
(113) Lakshmi, S.; Dutta, S.; Pati, S. K. *J. Phys. Chem. C* **2008**, *112*, 14718–14730.
(114) Mott, N. F.; Gurney, R. K. *Electronic Process in Ionic Crystals*; Clareton: Oxford, U.K., 1940.